



Research paper

Buckling resistance of metal columns with smoothly variable cross sections

Paweł Błażejowski¹, Tomasz Klekiel², Sebastian Kołodziej³,
Jakub Marcinowski⁴, Volodymyr Sakharov⁵

Abstract: Metal columns of hollow and smoothly variable cross-sections, simply supported at their ends are considered in the paper. Columns of such shapes are recently frequently designed by architects in public utility buildings of various types. In this work authors present the comparatively simple method of buckling resistance assessment which can be used by designers of metal columns of such shapes. The formula on critical force required in the procedure was derived for columns of variable cross section by means of Mathematica™ system. The closed formulae were obtained for a rod with a certain, predefined geometry being the surface of revolution. Critical forces obtained by means of derived formulae were compared with results of numerical solutions. To assess the compression resistance of considered rods the general Ayrton–Perry approach was applied and bow imperfection with assumed amplitude was used in the analysis. Results of numerical simulations and experimental tests inserted in the paper confirm the correctness and the effectiveness of the proposed procedure of buckling resistance assessment of considered struts.

Keywords: metal columns, variable cross section, buckling resistance, Ayrton–Perry approach, numerical simulations, experimental tests

¹PhD., Eng., University of Zielona Góra, Poland, Institute of Civil Engineering, Szafrana 1, 65-516 Zielona Góra, Poland, e-mail: p.blazejewski@ib.uz.zgora.pl, ORCID: 0000-0001-6369-7202

²DSc., PhD., Eng., University of Zielona Góra, Poland, Institute of Biomedical Engineering, Prof. Z. Szafrana 4, 65-516 Zielona Góra, Poland, e-mail: t.klekiel@iimb.uz.zgora.pl, ORCID: 0000-0002-2699-3528

³PhD., Eng., University of Zielona Góra, Poland, Institute of Civil Engineering, Szafrana 1, 65-516 Zielona Góra, Poland, e-mail: s.kolodziej@ib.uz.zgora.pl, ORCID: 0000-0002-2992-6021

⁴Prof., DSc., PhD., Eng., University of Zielona Góra, Poland, Institute of Civil Engineering, Szafrana 1, 65-516 Zielona Góra, Poland, e-mail: j.marcinowski@ib.uz.zgora.pl, ORCID: 0000-0001-6834-0843

⁵DSc., PhD., Eng., University of Zielona Góra, Poland, Institute of Civil Engineering, Szafrana 1, 65-516 Zielona Góra, Poland, e-mail: v.sakharov@ib.uz.zgora.pl, ORCID: 0000-0002-9381-3283

1. Introduction

Tapered columns resembling a spindle shape and fabricated as a steel, hollow sections are more and more often encountered in engineering practice (Fig. 1). Some of the main reasons for their increasing use are the material savings, a greater load capacity and aesthetic requirements [10, 11, 18]. Provisions of EN 1993 [5] do not offer direct procedures which can be used in designing of such kind of columns. Existing design procedures based on general Ayrton & Perry [3] approach refers only to columns of constant sections. This general approach requires knowledge of the critical force value and it is the principal problem which should be solved.

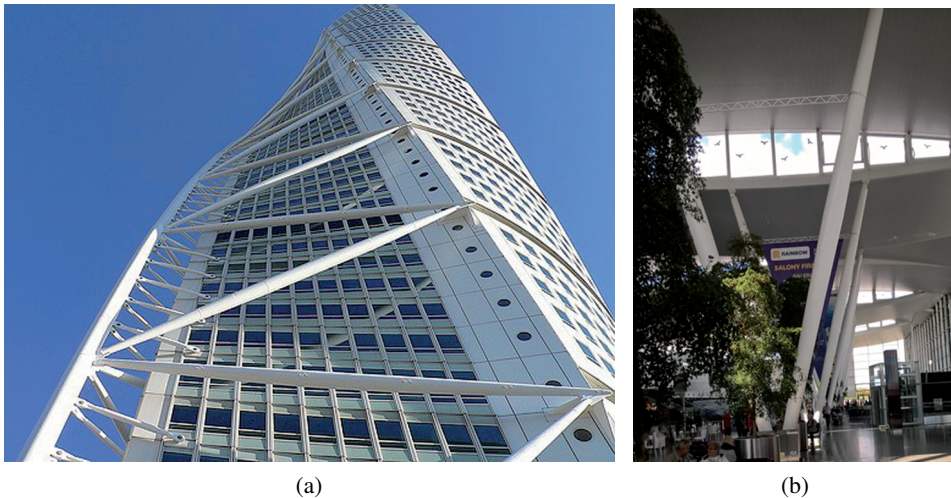


Fig. 1. Santiago Calatrava's "Turning Torso" in Malmö a), Wrocław Airport hall b)

There are a large number of papers in which the buckling problem of non-prismatic columns is considered [6, 8, 9]. Value of the critical forces is absolutely necessary to the assessment of load bearing capacity.

In the present paper the effective method of determination of the critical force has been presented. To this end the energetic criterion of stability proposed in Timoshenko & Gere [17] was used. The obtained analytical expression on the critical force has been verified positively by means of numerical solutions using commercial software based on finite element method.

To assess the compression resistance of the considered kind of columns the general Ayrton–Perry approach is adopted. This approach dating from XIX century [3], after many modifications, was inserted into contemporary design provisions [4] and used by many authors [7, 14, 15].

The stress criterion, in which the maximum stress was equated to the yield stress f_y in the most stressed section, was the condition from which the allowable compressive force was obtained. Similarly, as in the Ayrton–Perry approach, the initial bow imperfection has

been taken into account with the amplitude corresponding to the fabrication quality class. The effect of the eccentricity amplification, typical for slender compressed members, was taken into account as well. The stress condition has been checked in every section x along the column axis because, due to the column cross-section variability, it was not possible to predict in advance in which cross-section the stress condition will be decisive.

Only specific class of geometries of bulged column was considered in the paper. The effectiveness of the proposed designing procedure was illustrated on examples. They confirm the effectiveness of the proposed approach. Experimental tests carried out on specimens made of copper and presented in the paper also proved the correctness of the proposed procedure.

In authors' opinion the presented procedure can be used by engineers designing metal, bulged columns of the shape considered in the paper.

2. Derivation of formulae for the critical force

Due to the fact that columns of variable cross-sections are subject of interest in this work, the critical force can be established only in an approximate way using the energetic criterion of stability [17]. According to this criterion the critical force for pin ended column can be obtained from (2.1):

$$(2.1) \quad P_{cr} = E \cdot \int_0^L \left(\frac{dw(x)}{dx} \right)^2 dx \Bigg/ \int_0^L \frac{w(x)^2}{J(x)} dx$$

where: $w(x)$ – expected buckling form adopting here the shape of $1/2$ wave of sine function with the amplitude A_0 (Fig. 2), $J(x)$ – the moment of inertia of the cross section, E – the Young's modulus.

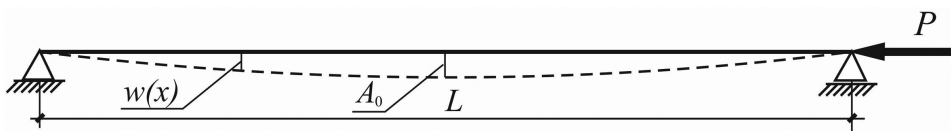


Fig. 2. Buckling mode of the pin ended compressed bar

Amplitude A_0 is irrelevant in these calculations as it is easy to see when analyzing formula (2.1). The moment of inertia $J(x)$ is defined in the following way (2.2):

$$(2.2) \quad J(x) = \frac{\pi}{4} [r(x)^4 - (r(x) - t)^4]$$

where: $r(x)$ – the external radius of variable cross section (comp. Fig. 3).

The external radius of variable cross section is defined as follows (2.3):

$$(2.3) \quad r(x) = \frac{D_1}{2} + \left(\frac{D_2}{2} - \frac{D_1}{2} \right) \cdot \sin \left(\frac{\pi \cdot x}{L} \right)$$

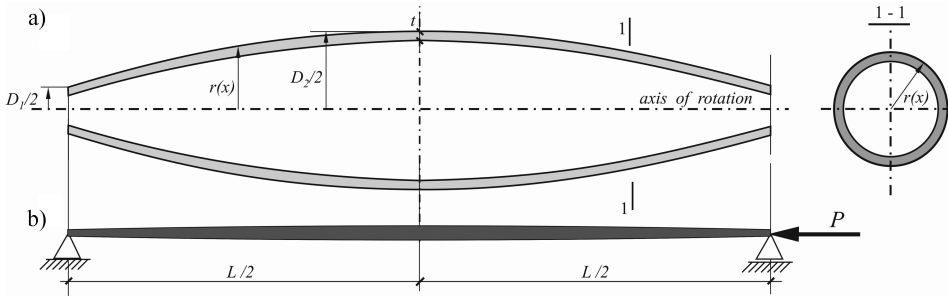


Fig. 3. Sections (scale not preserved) of the rod a) and static scheme of the compressed bar b)

where: D_1 – the external diameter of the terminal cross section, D_2 – the external diameter of the middle cross section, t – wall thickness, L – the length of the column.

Further considerations presented in this work were limited to some specific geometry defined uniquely by the column's length L . It was assumed that the external diameter of the terminal cross section is constant and equal $D_1 = 1/100L$. External diameters of the middle cross sections of considered bars adopt the following values $D_2/L = 4/200, 5/200, 6/200, 7/200, 8/200$. The wall thickness t is constant and adopts the following values: $t/L = 1/1000, 2/1000, 3/1000$. These particular geometrical parameters were used in further considerations.

Formulae expressing the critical forces for particular geometries of columns are presented in Table 1. They were obtained from (2.1) by means of derivations carried out in Mathematica™ system [20].

Table 1. Derived formulae on critical forces $P_{cr}/(E \cdot L^2)$

D_2/L	$t/L = 1/1000$	$t/L = 2/1000$	$t/L = 3/1000$
4/200	$1.91996 \cdot 10^{-8}$	$3.22130 \cdot 10^{-8}$	$4.05223 \cdot 10^{-8}$
5/200	$3.50317 \cdot 10^{-8}$	$6.03591 \cdot 10^{-8}$	$7.79138 \cdot 10^{-8}$
6/200	$5.71347 \cdot 10^{-8}$	$1.00223 \cdot 10^{-7}$	$1.31664 \cdot 10^{-7}$
7/200	$8.63133 \cdot 10^{-8}$	$1.53380 \cdot 10^{-7}$	$2.04083 \cdot 10^{-7}$
8/200	$1.23333 \cdot 10^{-7}$	$2.21330 \cdot 10^{-7}$	$2.97366 \cdot 10^{-7}$

To illustrate the procedure of obtaining P_{cr} for given data let us consider the case: $E = 210000 \text{ N/mm}^2$, $L = 1000 \text{ mm}$, $D_1 = L/100 = 10 \text{ mm}$, $D_2 = 2L/100 = 20 \text{ mm}$, $t = L/1000 = 1 \text{ mm}$. From the Table 1 we obtain $P_{cr} = 1.91996 \cdot 10^{-8} \cdot E \cdot L^2 = 4031.92 \text{ N} = 4.032 \text{ kN}$. This particular value appears in Table 2 and in example presented in Section 5.

3. Numerical verification of derived formulae on critical forces

The correctness of derived formulae was verified numerically by means of commercial software based on finite element method. Three different programs were used and two different models were created. The beam model was prepared in Autodesk® Robot™ Structural Analysis Professional system [2], the shell model was created in COSMOS/M system [4] while the 3D model was prepared in Simulia Abaqus system [1]. Details relating to particular finite elements used in analyses are presented in Section 5.

In the performed comparative analysis, the following data were adopted: $L = 1000$ mm, $D_1 = L/100 = 10$ mm, $E = 210000$ MPa (column made of steel). Results are presented in Table 2.

Table 2. Critical forces P_{cr} in [kN] obtained for the column of length $L = 1000$ mm

t [mm]	Calculation	$D_2 = 20$ m	$D_2 = 25$ mm	$D_2 = 30$ mm	$D_2 = 35$ mm	$D_2 = 40$ mm
1	Analytical	4.032	7.357	11.998	18.126	25.900
1	ROBOT	4.139	7.564	12.301	18.47	26.418
1	COSMOS	4.096	7.561	12.300	18.469	26.162
1	ABAQUS	4.158	7.561	12.373	18.584	26.364
2	Analytical	6.765	12.675	21.047	32.21	46.479
2	ROBOT	6.896	12.955	21.441	32.581	47.155
2	COSMOS	6.822	12.946	21.438	32.581	46.549
2	ABAQUS	6.946	13.032	21.678	32.931	47.095
3	Analytical	8.510	16.362	27.649	42.857	62.447
3	ROBOT	8.538	16.506	27.816	42.780	62.936
3	COSMOS	8.438	16.488	27.808	42.780	61.639
3	ABAQUS	8.748	16.819	28.424	43.647	62.897

Results presented in Table 2 confirm quite good correspondence between results obtained by means of derived formulae (labelled as Analytical) and results obtained numerically for the beam model (ROBOT), for the shell model (COSMOS/M) and for the 3D model (ABAQUS). The maximum deviations do not exceed 3.5%.

4. Resistance of the compressed column

The resistance of the considered strut will be assessed on the basis of classical Ayrton–Perry’s approach. Let us assume that the strut has an initial bow imperfection with amplitude e_0 (Fig. 4) in a form of the one half-wave sine function defined as follows (4.1):

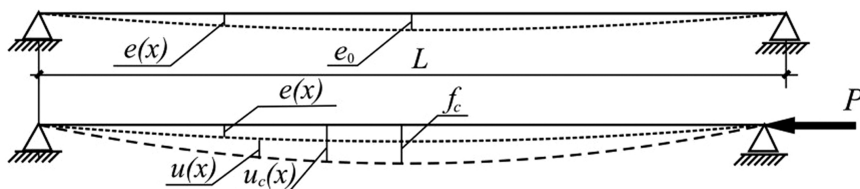


Fig. 4. Deflections of the initially curved rod

$$(4.1) \quad e(x) = e_0 \sin\left(\frac{\pi x}{L}\right)$$

The total deflection $u_c(x)$ can be obtained from the formula (4.2) (cf. [17]):

$$(4.2) \quad u_c(x) = f_c \sin\left(\frac{\pi x}{L}\right), \quad f_c = \frac{e_0}{1 - \frac{P}{P_{cr}}}$$

where: f_c – total eccentricity at middle section of the rod, P_{cr} – critical buckling force.

The maximum longitudinal stresses at arbitrary cross section defined by x can be calculated from the formula (4.3):

$$(4.3) \quad \sigma_{\max} = \frac{P}{A(x)} + \frac{P \cdot f_c}{W(x)} \cdot \sin\left(\frac{\pi \cdot x}{L}\right) \leq f_y$$

where: $A(x)$, $W(x)$ – are the cross sectional area and the elastic section modulus respectively, f_y – the yield stress.

The $A(x)$ and $W(x)$ can be obtained from formulae (4.4):

$$(4.4) \quad A(x) = \pi [r(x)^2 - (r(x) - t)^2] = \pi [2r(x)t - t^2], \quad W(x) = \frac{J(x)}{r(x)}$$

Using (4.2) and taking the equality in (4.3) we obtain:

$$(4.5) \quad \frac{P}{A(x)} + \frac{P}{W(x)} e_0 \cdot \frac{P_{cr}}{P_{cr} - P} \sin\left(\frac{\pi \cdot x}{L}\right) = f_y$$

To convert the equation (4.5) to the form known from EN1993-1-1 [5] let us introduce the notations:

$$(4.6) \quad P(x) = \chi(x) \cdot A(x) \cdot f_y, \quad \hat{\lambda}(x) = \sqrt{\frac{f_y A(x)}{P_{cr}}}$$

where: $\chi(x)$ – the buckling reduction factor, $\hat{\lambda}$ – the non-dimensional slenderness, both dependent on x .

Substituting (4.6) to eqn. (4.5) and introducing the quantity $\Phi(x)$ defined as follows (4.7):

$$(4.7) \quad \Phi(x) = \frac{1}{2} \left[1 + \frac{A(x)}{W(x)} e_0 \cdot \sin\left(\frac{\pi \cdot x}{L}\right) + \hat{\lambda}^2(x) \right]$$

one obtains the equation (4.8):

$$(4.8) \quad \chi^2(x) \cdot \hat{\lambda}^2(x) - \chi(x) \cdot 2\Phi(x) + 1 = 0$$

from which the searched reduction factor $\chi(x)$ is obtained in the form (4.9):

$$(4.9) \quad \chi(x) = \frac{\Phi(x) - \sqrt{\Phi^2(x) - \hat{\lambda}^2(x)}}{\hat{\lambda}^2(x)} = \frac{1}{\Phi(x) + \sqrt{\Phi^2(x) - \hat{\lambda}^2(x)}}$$

which is consistent with the formula (6.49) from EN 1993-1-1 [5] valid for columns of constant cross-section.

The column's resistance P_{ult} is determined by the smallest value of the expression (4.10):

$$(4.10) \quad P_{ult}(x) = \chi(x) \cdot A(x) \cdot f_y$$

The value of ultimate force defined by formulae (4.10) could be too high in some circumstances. For save design procedures the additional partial safety coefficient $\gamma = 1.2$ is proposed and the final formula for design value of column's resistance is as follows (4.11):

$$(4.11) \quad P_{Rd}(x) = \frac{1}{\gamma} \cdot \chi(x) \cdot A(x) \cdot f_y$$

where: γ – the partial safety factor.

The whole procedure can be easily inserted in spreadsheet for every x from the interval $0 < x < L/2$, and in this way the smallest value of P_{Rd} can be found.

The initial bow amplitude e_0 required in this procedure can be adopted according to the code recommendations. Following provisions inserted in Eurocodes specifying tolerances, dimensions and sectional properties of steel structural elements the e_0 can be adopted as $L/750$ and this value guaranteeing the conservative assessment of columns resistance was adopted in examples presented in the next section.

5. Examples

As the first example of the application of presented procedure let us consider the bulged, steel bar of length $L = 1000$ mm, $D_1 = L/100 = 10$ mm, $D_2 = 2L/100 = 20$ mm, $t = L/1000 = 1$ mm and $e_0 = L/750 = 1.333$ mm. Material parameters: $E = 210$ MPa, the yield stress $f_y = 355$ MPa.

The critical force calculated by means of the formula (cf. Table 1) is $P_{cr} = 4.032$ kN. Using the spreadsheet, the sequence of P_{ult} were calculated from the formula (4.11) for $x = 0$ to 500 ($L/2$) with step 5 mm. The smallest value of the compression force $P_{ult, \min} = 3.766$ kN and this value was obtained for $x = 220$ mm. The column's design resistance calculated from the formula (4.11) is equal $P_{Rd} = 3.138$ kN and it is the searched measure of the bar's compression resistance.

The same example was solved numerically by means of Abaqus system. Two kind of modelling were adopted in numerical simulations which were carried out and namely the shell model (63126 DOF) and the 3D (solid) model (94695 DOF). In the first case, the S4 type of shell finite element was used, which uses thick shell theory and include four internal integration points. With the solid model used C3D8I type of solid finite element's family with ("incompatible modes"). These elements have additional internal degrees of freedom (incompatible deformation modes) eliminating "parasitic shear stresses" and the shear-locking phenomena described in [21]. Using these models for 1/4 of the column (the column had two planes of symmetry) the geometrically and materially nonlinear analysis with imperfections (GMNIA) was performed. The uniformly distributed load was applied at the columns end. The bilinear material model for steel was adopted. Equilibrium paths obtained by two models were nearly identical (less than 2%) which confirms the correctness of the simulation performed.

The $\sigma_x = 355$ MPa appeared at section $x = 237.5$ mm (comp. Fig. 5) when the load attained value $P = 3.874$ kN. It is the value 2.5% higher than the result obtained with the analytical method. The maximum load on the equilibrium path was equal $P_{max} = 3.883$ kN. The design value of column's resistance was equal $3.874/1.2 = 3.23$ kN and this level was shown in Fig. 5.

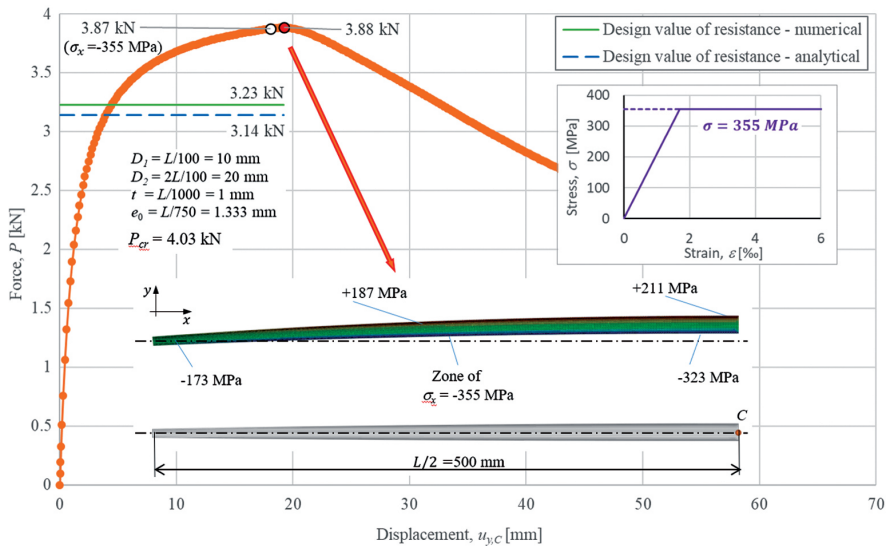


Fig. 5. Nonlinear equilibrium path obtained in numerical simulation

As the other example let us consider the column of following parameters: $D_2 = 4L/100 = 40$ mm, $t = 3L/1000 = 3$ mm. Remaining geometrical and material parameters were the same.

The critical force calculated by means of the formula (Table 1) is $P_{cr} = 62.447$ kN. In this case the $P_{ult,min} = 23.421$ kN and this value was obtained for $x = 0$ mm (column's end). The column's design resistance calculated from the formula (4.11) is equal

$P_{Rd} = 18.45$ kN. The counterpart of this value obtained numerically was equal 18.66 kN. Fig. 6 presents a comparison of numerical simulations with the buckling resistance assessment proposed in Section 4.

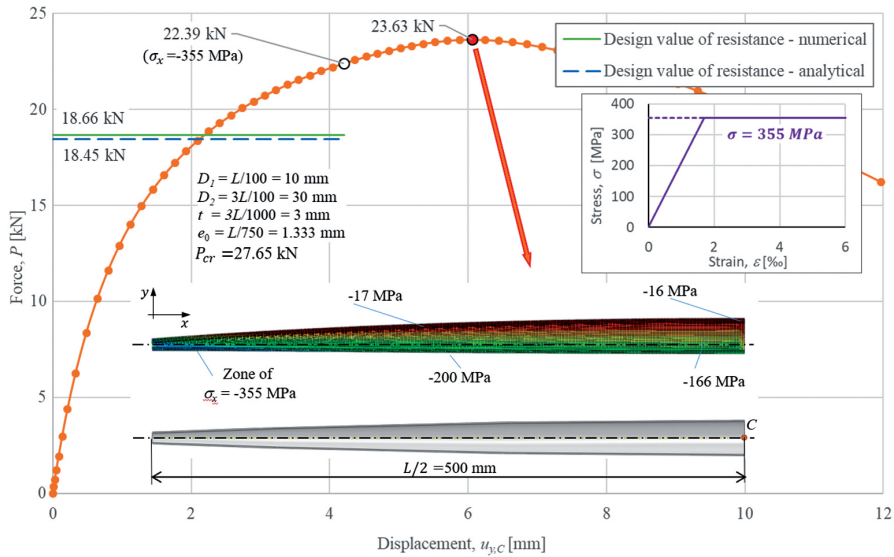


Fig. 6. Nonlinear equilibrium path obtained in numerical simulation

In both examples the column's design resistances obtained analytically were conservative.

6. Experimental tests supported by numerical simulations

6.1. Experimental tests

In order to confirm the effectiveness of the proposed procedure experimental tests were carried out. Due to some difficulties in manufacturing the steel specimen, it was made of copper sheet. Detailed geometrical parameters of specimen were presented in Fig. 7. Due to symmetry, only half of the specimen was shown in the figure.

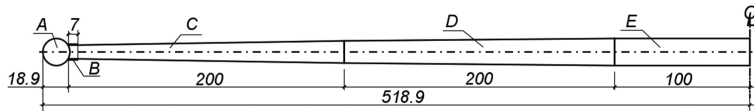


Fig. 7. Nominal geometrical parameters of the specimen: A – steel ball, $\phi = 20$ mm, B – reinforcement collar, $t = 1$ mm, C – conical part: $\phi_{\text{ext}} = 10$ mm to $\phi_{\text{ext}} = 16.4$ mm, D – conical part: $\phi_{\text{ext}} = 16.4$ mm to $\phi_{\text{ext}} = 20$ mm, E – cylindrical part: $\phi_{\text{ext}} = 20$ mm

Surfaces of specimens were covered by spot patterns required to displacement measurements based on 3D digital image correlation (DIC) method (comp. Fig. 8).

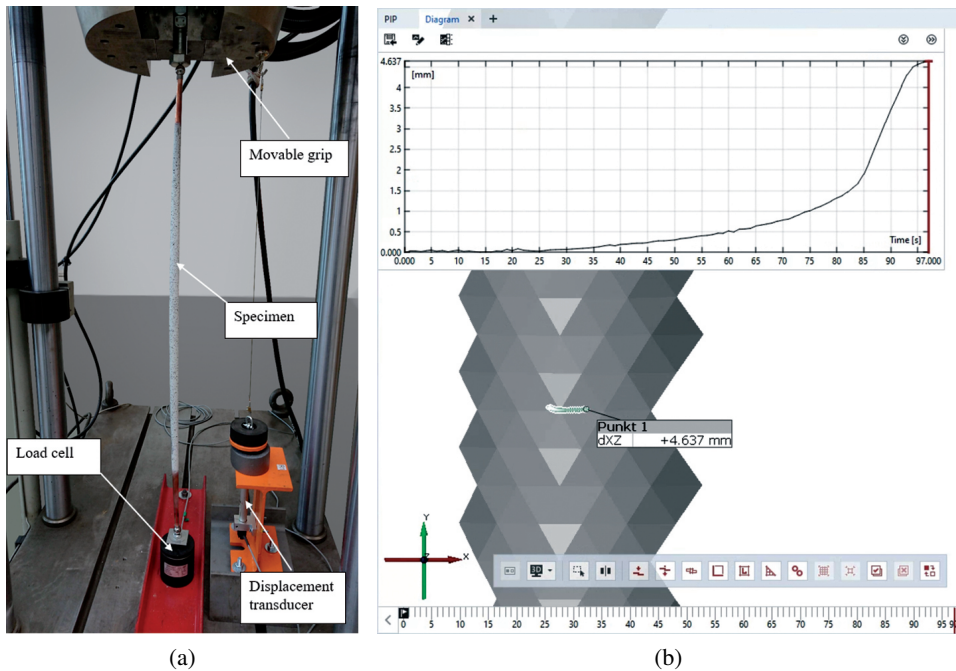


Fig. 8. Specimen during the compression test a), snapshot from *GOM Correlate software* with trajectory curve and lateral displacement diagram b)

In general, the DIC technology makes it possible to scan the geometry of the visible part of the surface and its changes during the deformation by optical digital cameras. This technology provides precise notation of the spatial (3D) displacement of surface points with subsequent analysis of displacements, deformations, etc. This technology can be used to identify some mechanical parameters or making comparative analyses with numerical simulations [13, 16]. In this work, DIC was used to measure the magnitude of lateral displacements (in an arbitrary direction) of the middle point of the beam during the compressive test. Computer processing was carried out using *GOM Correlate software* (comp. Fig. 8b).

Specimens were manufactured from the copper sheet of thickness $t = 0.3$ mm. Coupons of this material were used to detect material characteristics. Particular parts of specimen were connected to each other by tin welds. Terminal parts of specimens were reinforced by collars made of zinc sheet of thickness $t = 1$ mm. To simulate pin ended boundary conditions of examined columns their ends were supported by steel balls (comp. Fig. 7 and Fig. 8).

To obtain material characteristic, tensile tests were made on six coupons cut from the copper sheet. The exemplary stress-strain characteristic was presented in Fig. 9 in which also best fit characteristic obtained by means Mathematica™ [20] was shown. In this figure

also the $\sigma_{\text{true}}(\varepsilon_{\text{true}})$ plot was shown in accordance with formula (C.1) from EN1993-1-5. Within considered range of stresses the $\sigma(\varepsilon)$ relationship is nearly identical to the $\sigma_{\text{true}}(\varepsilon_{\text{true}})$ plot. The best fit nonlinear characteristic in a form presented in Fig. 9 was used in numerical simulations.

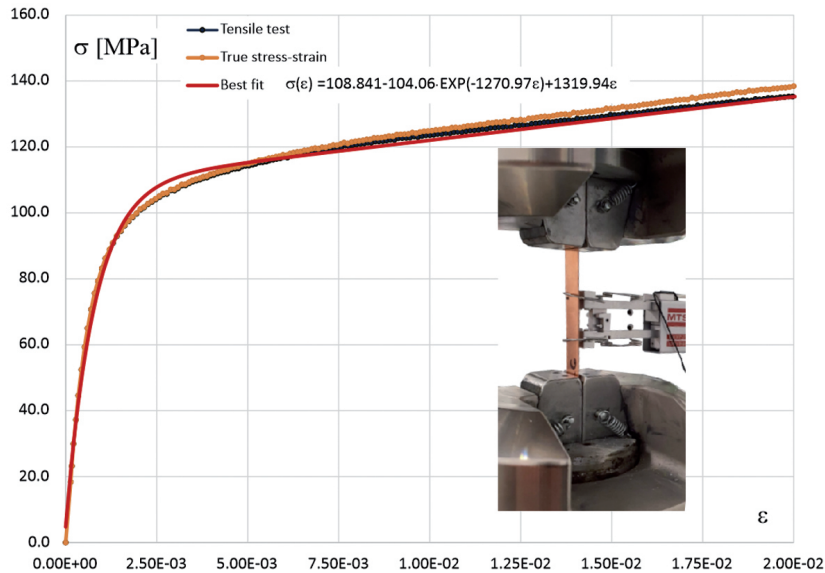


Fig. 9. Stress-strain characteristic

It is seen that stress-strain relation is strongly nonlinear. As the yield stress the average value of $R_{0.02}$ was adopted and in the case of tested material it was equal 107.3 MPa.

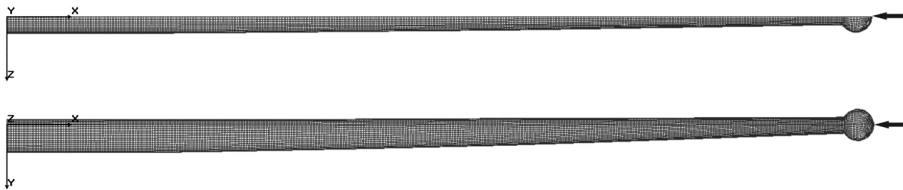
Fig. 8a presents the specimen on the test rig during compression test. Lateral displacements were measured by means the DIC technique. Two cameras make possible to register spatial motion of dots located in neighbourhood of middle segment of the specimen. Vertical displacements of the upper end were measured by the inductive displacement transducer arranged in the way shown in Fig. 8a. The test was carried out in such a manner that the grip of the hydraulic test machine was being moved downward with very slow motion (1 mm/min). During the test the compression force was measured by the load cell (comp. Fig. 8a) and characteristic displacements were registered at the same instants. Sampling rates were equal to 1 sps (sample per second) in a case of picture registration and 4 sps in a case of load and axial displacements acquisition. As a result, the whole load displacement paths were obtained. The maximum load on these paths were the measure of buckling resistances of tested specimens. Results obtained for three tested specimens were shown together with results of numerical simulations in Fig. 11. Initial segments of obtained nonlinear equilibrium paths were used to determine critical forces P_{cr} required in the procedure presented in Section 4. To this end the Southwell's method [12] was used. Critical forces obtained by this way for three specimens were shown in Table 3.

Table 3. Critical forces P_{cr} obtained in laboratory tests

Parameter	Specimen's identification		
	PM1	PM2	PM3
P_{cr} [N]	745.10	737.75	791.49
$P_{cr,average}$ [N]	758.11		

6.2. Numerical simulations

Numerical simulations of compression tests were carried out by means of COSMOS/M system based on FEM [4]. Column's geometry was discretized by means of quadrilateral finite elements with six degrees of freedom at nodes. Due to double symmetry only one quarter of the specimen was discretized and the discrete model was defined by 11531 elements and 12068 nodes which led to discrete model with 72408 degrees of freedom. Appropriate boundary conditions were superimposed: clamped middle section and symmetry conditions on $x - y$ surface (Fig. 10). The concentrated load was applied at terminal node of the steel ball.

Fig. 10. Discrete model of the strut quarter with bow imperfection of amplitude $L/150$

Five different modes of initial imperfections were considered. These were bow imperfections with amplitudes: $f = L/150$, $L/400$, $L/500$, $L/1000$, $L/2000$, $L/5000$.

The critical value of load couldn't be obtained by the method presented in Section 2 due to the fact that the Young's modulus was not constant as it was in case of steel. To obtain the critical buckling force for considered columns of ideal geometry, the Southwell's approach was adopted [12]. To this end the initial segments of equilibrium paths obtained numerically were used. Results of the Southwell's approach were presented in Table 4.

Table 4. Critical forces P_{cr} obtained in laboratory tests

Parameter	Imperfection case					
	$f = l/150$	$f = l/400$	$f = l/500$	$f = l/1000$	$f = l/2000$	$f = l/5000$
P_{cr} [N]	792.48	812.75	808.08	792.87	806.84	801.27
$P_{cr,average}$ [N]	802.38					

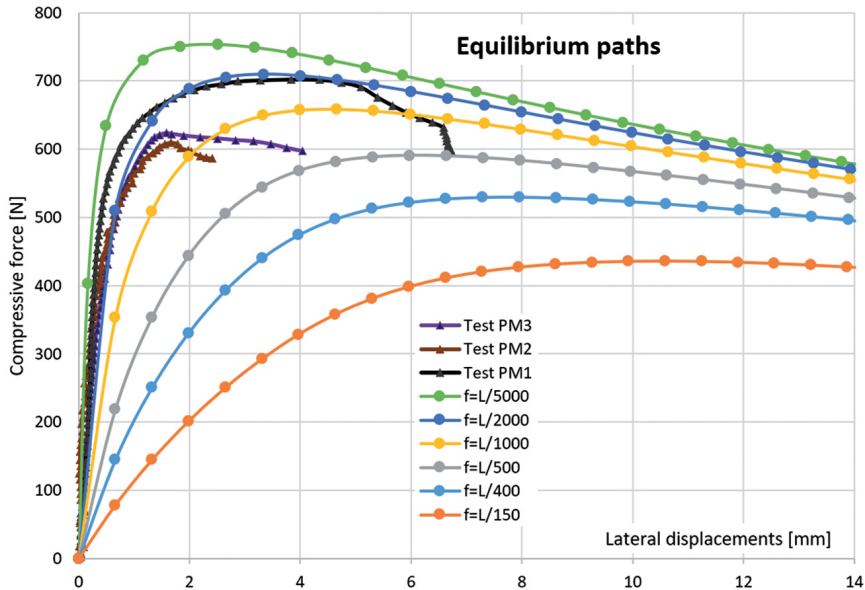


Fig. 11. Equilibrium paths: test results and numerical simulations

The average value $P_{cr} = 803.4$ N was used in the procedure presented in Section 4. As the yield stress the value obtained in material tests as $R_{0.02} = 107.3$ MPa was adopted. The statement of all obtained results was presented in Table 5.

Table 5. Buckling resistances of considered copper struts

Case	P_{max} [N]	P_{Rk} [N]	P_{Rd} [N]
1	2	3	4
$f = L/150$	436.1	453.5	377.9
$f = L/400$	529.9	600.5	500.4
$f = L/500$	590.7	627.8	523.2
$f = L/1000$	658.8	695.8	579.8
$f = L/2000$	709.6	741.4	617.8
$f = L/5000$	753.3	775.1	645.9

Buckling resistances for particular cases of struts obtained numerically were presented in column no. 2. Characteristic values of resistances obtained by the method presented in Section 4 was given in column no. 3. Design values of resistances obtained from eqn. (4.11) was presented in column no. 4.

Buckling resistances obtained in experimental tests were equal respectively: 702.4 N (PM1), 609.6 N (PM2), 623.4 N (PM3). One can expect that the fabrication quality of

examined struts corresponds to amplitude of bow imperfections on the level $L/1000$ – $L/2000$.

It is worth emphasizing that the design values of the load capacity calculated using the method proposed in Section 4 are lower than the resistances obtained numerically and experimentally and it confirms its conservative character.

7. Recapitulation and conclusions

Existing design regulations do not contain provisions for design of steel, compressed members of structures when they are non-prismatic. Authors have presented the procedure which allows determining the critical force for non-prismatic rods of specific geometry. Knowing the critical force one can assess the compression resistance of the rod under consideration using the other, based on Ayrton–Perry approach, procedure details of which were presented in the paper. Due to the fact that the cross section is variable, the stress criterion which follows from Ayrton–Perry condition should be checked not only in middle section of the bar but also in all remaining cross-sections. This stage of the procedure can be accomplished easily by means of the spreadsheet in which formulae presented in this paper should be inserted for arbitrary value of the axial coordinate x of the rod. The smallest value of compression force obtained as the result of the presented procedure is the measure of compression resistance of the considered rod.

Examples presented in the paper confirm that the proposed procedure is relatively easy, effective and correct what was proved in geometrically and materially nonlinear numerical simulations presented in the paper. Experimental tests and numerical simulations made on struts made of copper confirm the positive features of the presented approach to the buckling resistance assessment of metal columns of variable cross section. The presented design procedure can be recommended for civil engineers designing metal, structural members of the particular shape considered by authors. The design value of compressive force obtained as a final result of the procedure can be treated as a compressive resistance of analysed columns. The presented proposal effectively fills the gap existing in the available design recommendations.

References

- [1] Massachusetts Institute of Technology, “Abaqus Documentation”, 2020. [Online]. Available: <https://abaqus-docs.mit.edu/2017/English/SIMACAEEEXCRefMap/simaexc-c-docproc.htm>. [Accessed: 3.03.2020].
- [2] Autodesk Robot Structural Analysis Professional, *User's manual*. 2016.
- [3] W. E. Ayrton, and J. Perry, “On struts”, *The Engineer*, vol. 62, pp. 464–465, 1886.
- [4] COSMOS/M, *Finite Element Analysis System, Version 2.9*. Structural Research and Analysis Corporation, Electronic Manual, Los Angeles, California, 2002.
- [5] EN 1993-1-1:2005 Eurocode 3: Design of steel structures – Part 1–1: General rules and rules for buildings. CEN, Brussels, 2005.
- [6] I. Elishakoff, and O. Rollot, “New closed-form solutions for buckling of a variable stiffness column by mathematical”, *Journal of Sound and Vibration*, vol. 224, no. 1, pp. 172–82, 1999, doi: 10.1006/JSVI.1998.2143.

- [7] M. A. Giżejowski, Z. Stachura, R. B. Szczerba, and M. D. Gajewski, “Buckling resistance of steel H-section beam—columns: In-plane buckling resistance”, *Journal of Constructional Steel Research*, vol. 157, pp. 347–358, 2019, doi: [10.1016/J.JCSR.2019.03.002](https://doi.org/10.1016/J.JCSR.2019.03.002).
- [8] Q. S. Li, H. Cao, and G. Li, “Stability analysis of bars with varying cross-section”, *International Journal of Solids and Structures*, vol. 32, no. 21, pp. 3217–3228, 1995.
- [9] Q. S. Li, “Exact solutions for buckling of non-uniform columns under axial concentrated and distributed loading”, *European Journal of Mechanics – A/Solids*, vol. 20, no. 3, pp. 485–500, 2001, doi: [10.1016/S0997-7538\(01\)01143-3](https://doi.org/10.1016/S0997-7538(01)01143-3).
- [10] J. Marcinowski, “Maximum elastic buckling resistance of columns of constant volume”, presented at XIV Stability of structures XIV-th Symposium, Zakopane, 08–12 June, 2015.
- [11] J. Marcinowski and M. Sadowski, “Using the ERFI function in the problem of the shape optimization of the compressed rod”, *International Journal of Automotive and Mechanical Engineering*, vol. 25, no. 2, pp. 75–87, 2020, doi: [10.2478/ijame-2020-0021](https://doi.org/10.2478/ijame-2020-0021).
- [12] J. Marcinowski M. Sadowski, and V. Sakharov, “On the applicability of Southwell’s method to the determination of the critical force of elastic columns of variable cross sections”, *Acta Mechanica*, vol. 233, pp. 4861–4875, 2022, doi: [10.1007/s00707-022-03345-w](https://doi.org/10.1007/s00707-022-03345-w).
- [13] P. Romanowicz, B. Szybiński, and M. Wygoda, “Application of DIC method in the analysis of stress concentration and plastic zone development problems”, *Materials*, vol. 13, no. 16, art. no. 3460, 2020, doi: [10.3390/ma13163460](https://doi.org/10.3390/ma13163460).
- [14] J. Szalai and F. Papp, “On the theoretical background of the generalization of Ayrton–Perry type resistance formulas”, *Journal of Constructional Steel Research*, vol. 66, no. 5, pp. 670–679, 2010, doi: [10.1016/j.jcsr.2009.12.013](https://doi.org/10.1016/j.jcsr.2009.12.013).
- [15] J. Szalai, “Complete generalization of the Ayrton–Perry formula for beam-column buckling problems”, *Engineering Structures*, vol. 153, no. 15, pp. 205–223, 2017, doi: [10.1016/j.engstruct.2017.10.031](https://doi.org/10.1016/j.engstruct.2017.10.031).
- [16] I. Szewczak, K. Rzeszut, P. Rozyło, and S. Samborski, “Laboratory and numerical analysis of steel cold-formed sigma beams retrofitted by bonded CFRP tapes”, *Materials (Basel)*, vol. 13, no. 19, art. no. 4339, 2020, doi: [10.3390/ma13194339](https://doi.org/10.3390/ma13194339).
- [17] S. Timoshenko and J. Gere, *Theory of elastic stability*. New York: McGraw-Hill, 1961.
- [18] P. Thompson, G. Papadopoulou, and E. Vassiliou, “The origins of entasis: illusion, aesthetics or engineering?”, *Spatial Vision*, vol. 20, no. 6, pp. 531–543, 2007, doi: [10.1163/156856807782758359](https://doi.org/10.1163/156856807782758359).
- [19] B. Turoń, D. Ziaja, L. Buda-Ożóg, and B. Miller, “DIC in validation of boundary conditions of numerical model of reinforced concrete beams under torsion”, *Archives of Civil Engineering*, vol. 64, no. 4/II, pp. 31–48, 2018, doi: [10.2478/ace-2018-0061](https://doi.org/10.2478/ace-2018-0061).
- [20] S. Wolfram, *Mathematica™, A system for doing mathematics by computer*. Addison-Wesley Publishing Company, Inc., 1988.
- [21] D. Xu, R. Xiao, Y. Wang, and D. Ling, “Eight-node shell element based on incompatible modes”, *Communications in Numerical Methods in Engineering*, vol. 25, no. 2, pp. 103–119, 2009, doi: [10.1002/cnm.1108](https://doi.org/10.1002/cnm.1108).

Nośność wyboczeniowa słupów metalowych o płynn timer zmiennym przekroju poprzecznym

Słowa kluczowe: słupy metalowe, zmienny przekrój pierścieniowy, siła krytyczna, metoda Ayrtona-Perry’ego, symulacje numeryczne, badania eksperymentalne

Streszczenie:

Przedmiotem rozważań zaprezentowanych w artykule są słupy metalowe o przekroju pierścieniowym zmiennym wzdłuż ich osi wzdłużnej i swobodnie podpartych na końcach. Słupy tego kształtu są ostatnio często projektowane przez architektów w różnego typu obiektach użyteczności publicznej.

Relatywnie prosty sposób oszacowania nośności wyboczeniowej słupów rozważanego kształtu został zaprezentowany przez autorów pracy. Wzór na siłę krytyczną niezbędną do oszacowania nośności wyboczeniowej został wyprowadzony z wykorzystaniem systemu Mathematica™. Zamknięte wzory na siły krytyczne zostały wyprowadzone dla pewnej klasy prętów o wstępnie zdefiniowanej geometrii stanowiącej powierzchnię obrotową. Siły krytyczne otrzymane z pomocą wyprowadzonych wzorów były porównane z wynikami symulacji numerycznych. Aby oszacować nośność wyboczeniową zastosowano ogólne podejście Ayrton–Perry’ego i wstępne wygięcie łukowe prętów o założonych różnych amplitudach. Wyniki symulacji numerycznych i badań eksperymentalnych zamieszczone w pracy potwierdziły poprawność i efektywność zaproponowanej metody szacowania nośności wyboczeniowej rozważanych prętów.

Received: 2022-12-21, Revised: 2023-01-31